




ORIGINAL RESEARCH

Computerized Analysis of the Ventricular Fibrillation Waveform Allows Identification of Myocardial Infarction: A Proof-of-Concept Study for Smart Defibrillator Applications in Cardiac Arrest

Jos Thannhauser , MSc; Joris Nas , MD; Dennis J. Rebergen, MSc; Sjoerd W. Westra , MD; Joep L. R. M. Smeets, MD, PhD; Niels Van Royen, MD, PhD; Judith L. Bonnes, MD, PhD; Marc A. Brouwer, MD, PhD

BACKGROUND: In cardiac arrest, computerized analysis of the ventricular fibrillation (VF) waveform provides prognostic information, while its diagnostic potential is subject of study. Animal studies suggest that VF morphology is affected by prior myocardial infarction (MI), and even more by acute MI. This experimental in-human study reports on the discriminative value of VF waveform analysis to identify a prior MI. Outcomes may provide support for in-field studies on acute MI.

METHODS AND RESULTS: We conducted a prospective registry of implantable cardioverter defibrillator recipients with defibrillation testing (2010–2014). From 12-lead surface ECG VF recordings, we calculated 10 VF waveform characteristics. First, we studied detection of prior MI with lead II, using one key VF characteristic (amplitude spectrum area [AMSA]). Subsequently, we constructed diagnostic machine learning models: model A, lead II, all VF characteristics; model B, 12-lead, AMSA only; and model C, 12-lead, all VF characteristics. Prior MI was present in 58% (119/206) of patients. The approach using the AMSA of lead II demonstrated a C-statistic of 0.61 (95% CI, 0.54–0.68). Model A performance was not significantly better: 0.66 (95% CI, 0.59–0.73), $P=0.09$ versus AMSA lead II. Model B yielded a higher C-statistic: 0.75 (95% CI, 0.68–0.81), $P<0.001$ versus AMSA lead II. Model C did not improve this further: 0.74 (95% CI, 0.67–0.80), $P=0.66$ versus model B.

CONCLUSIONS: This proof-of-concept study provides the first in-human evidence that MI detection seems feasible using VF waveform analysis. Information from multiple ECG leads rather than from multiple VF characteristics may improve diagnostic accuracy. These results require additional experimental studies and may serve as pilot data for in-field smart defibrillator studies, to try and identify acute MI in the earliest stages of cardiac arrest.

Key Words: amplitude spectrum area ■ cardiac arrest ■ machine learning ■ myocardial infarction ■ ventricular fibrillation

Ventricular fibrillation (VF) is the presenting heart rhythm in about 30% of out-of-hospital cardiac arrests (OHCAs), with dismal survival despite improvements in the chain of care.^{1,2} With the emerging applications of artificial intelligence, new strategies have been suggested to try and improve cardiac arrest

care, involving computerized VF waveform analysis of the paddle ECG.³

The amplitude spectrum area (AMSA) of the VF waveform has become the key characteristic of interest in prognostic studies on defibrillation success and neurological outcome.^{3–6} Moreover, a current

Correspondence to: Jos Thannhauser, MSc, Department of Cardiology 616, Radboud University Medical Center, P.O. Box 9101, 6500 HB Nijmegen, The Netherlands. E-mail: Jos.thannhauser@radboudumc.nl or j.thannhauser@outlook.com

Supplementary Materials for this article are available at <https://www.ahajournals.org/doi/suppl/10.1161/JAHA.120.016727>

For Sources of Funding and Disclosures, see page 9.

© 2020 The Authors. Published on behalf of the American Heart Association, Inc., by Wiley. This is an open access article under the terms of the Creative Commons Attribution-NonCommercial-NoDerivs License, which permits use and distribution in any medium, provided the original work is properly cited, the use is non-commercial and no modifications or adaptations are made.

JAHA is available at: www.ahajournals.org/journal/jaha

CLINICAL PERSPECTIVE

What Is New?

- Computerized analysis of the ventricular fibrillation (VF) waveform can be used for prognostication, but its diagnostic utility has so far been investigated only in animal studies.
- This is the first in-human VF waveform study that demonstrates the diagnostic performance, in terms of detection of underlying prior myocardial infarction (MI).
- With use of machine learning models, we showed that the diagnostic accuracy was better with multiple ECG leads than with a single-lead approach.

What Are the Clinical Implications?

- Animal studies have demonstrated that acute MI results in more apparent changes in VF morphology than prior MI.
- Therefore, this in-human study on prior MI provides pilot data for future in-field studies, to detect acute MI with defibrillator-guided VF waveform analysis.
- If proven feasible, in-field detection of an acute MI during VF could optimize triage and treatment in the earliest stages of cardiac arrest.

Nonstandard Abbreviations and Acronyms

AMSA	amplitude spectrum area
DFA	detrended fluctuation analysis
OHCA	out-of-hospital cardiac arrest
SVM	support vector machine

international randomized trial studies the impact of a smart defibrillator that provides real-time AMSA analysis and guides defibrillation timing, with the aim to improve outcomes.⁷

Another application of the VF waveform could be identification of the underlying arrest cause. With the introduction of advanced resuscitative therapies (eg, mechanical cardiopulmonary resuscitation, extracorporeal life support), early transportation and intervention has become possible.⁸ Such “early invasive” strategies in particular may be beneficial for patients with an underlying acute myocardial infarction (MI).^{9–11}

For such strategies, very early recognition of acute MI is crucial, while at present the diagnosis of acute MI is restricted to patients who (eventually) achieve return of spontaneous circulation.^{12,13} Studies in animals have shown that the appearance of the VF waveform is affected by ischemia¹⁴ and by prior MI, and that changes are even more impressive in acute MI.^{14–16} In human

studies in the setting of OHCA, it has been shown that AMSA values were lower in patients with than without ST-segment–elevation MI.^{17,18}

In follow-up on these observed associations, we sought to assess whether VF waveform analysis of the surface ECG may also facilitate detection of an MI. Given the logistical challenges of an in-field study on the diagnostic performance of acute MI, we designed a proof-of-concept study in the setting of defibrillation testing after implantable cardioverter defibrillator (ICD) implantations and focused on detection of a prior MI.^{16,19,20} First, we assessed the feasibility of MI identification using the AMSA of lead II, which has been used as a proxy for the paddle ECG signal in previous VF waveform studies.^{21–23} Moreover, we investigated whether the diagnostic accuracy could be improved by combinations of VF characteristics or the use of additional ECG leads, using machine learning discriminative models.

METHODS

Data Transparency Statement

Requests to access the anonymized data set from qualified researchers trained in human subject confidentiality protocols may be sent to the corresponding author of this article.

Patient Population

From our prospective registry of first ICD implantations at the Radboud University Medical Center (Nijmegen, The Netherlands), we identified all patients who underwent defibrillation testing between 2010 and 2014, which was the hospital protocol during that period. For the present analyses, we included patients with an analyzable 12-lead surface ECG of induced VF. Exclusion criteria were age <18 years, congenital heart disease, right-sided ICDs, and subcutaneous ICDs. In line with our previous publication, patients were excluded in case of a history of MI that did not involve the anterior or inferior wall.²⁰ Given the observational design of the study, written informed consent was not necessary to obtain according to the Dutch Act on Medical Research Involving Human Subjects.

ICD Implantation and Testing

The devices implanted were Medtronic (Minneapolis, MN), St Jude Medical (St. Paul, MN), or Biotronik (Berlin, Germany) ICD or cardiac resynchronization therapy defibrillator systems with transvenous single-coil leads. Defibrillation testing was performed after ICD implantation to test the ability of the implanted device to sense, detect, and terminate VF

appropriately. Following our hospital protocol, patients were sedated with propofol, after which VF was induced using T-wave shock, direct current pulses, or 50-Hz burst pacing. The presence of VF, defined as a rapid (around 300 bpm) grossly irregular ventricular rhythm with marked variability in QRS cycle length, morphology, and amplitude, was confirmed on surface ECG recordings. ICDs were programmed to deliver sequential shocks (15–25–35 J) until VF was terminated. In case of persisting VF after 3 shocks, external defibrillation was performed.

Aim of the Study

The primary aim of this study was to discriminate between patients with and without a prior MI with VF waveform information from lead II, using either an AMSA-only approach or a combination of VF features. Subsequently, we assessed and compared the discriminative performance of VF waveform analysis with data input of 12 ECG leads, using either the AMSA or combined VF features.

Study Groups

Patients were divided in 2 groups, either with or without a history of MI. For the present analyses, we used the study groups as reported on previously.²⁰ In short, MI was defined according to the criteria of the European Society of Cardiology.²⁴ Evidence for the presence or absence of a prior MI was based on reports in the medical charts.^{20,24} Infarct localization was based on information obtained from ECGs (eg, area with ST-segment elevation or pathological Q waves) and coronary angiographies, and confirmed by imaging reports.^{24,25} Imaging was performed and analyzed as part of daily clinical practice, following recommendations of the prevailing guidelines for ICD therapy.^{20,26}

VF Waveform Analysis

ECG Recordings

During defibrillation testing, a standard 12-lead surface ECG was recorded (sampling frequency, 1000 Hz; 16-bit analog-to-digital converter) with BARD LabSystem (Lowell, MA).

VF Waveform Characteristics

All definitions, mathematical descriptions and VF waveform calculations are described in more detail in Data S1. Signal analysis was performed using Matlab (version R2018a, The Mathworks Inc, Natick, MA). A VF segment of 4.1 seconds (4096 samples) directly before the first ICD shock was selected for waveform analysis. Signals were preprocessed with a fourth-order

Butterworth 1- to 48-Hz bandpass filter, after which VF waveform characteristics were calculated. We analyzed 10 different VF waveform characteristics, which can be categorized into *time domain* characteristics, *frequency domain* characteristics, and *signal organization* characteristics.

1. Time domain: From the filtered ECG segment in the time domain, we determined the amplitude of the VF signal,²⁷ more specifically defined as the mean absolute amplitude.²⁰ Moreover, we calculated the median slope,²⁸ which can be regarded as a measure of the overall steepness of the VF signal.
2. Frequency domain: After conversion of the ECG segment to the frequency domain using a fast Fourier transform, the AMSA²⁹ was calculated as the summed product of individual frequencies and their corresponding amplitudes over an interval of 2 to 48 Hz, a frequency range that is also used in the key AMSA paper.³ Subsequently, the power spectrum was obtained, from which the power spectrum area²⁸ was calculated. Moreover, we determined the dominant frequency,³⁰ which is the frequency where the power spectrum attains its maximum, and the median frequency,³¹ that is, the frequency for which the integrated power was half of the total integrated power. Finally, we calculated the bandwidth, defined as the frequency difference between the first and third quartile of the total power, providing a measure of the spread in frequencies.³²
3. Signal organization: The organization index³³ was calculated as the sum of the power of the dominant frequency and its harmonics, divided by the total power of the signal, over an interval of 2 to 48 Hz (Figure S1).¹⁹ Furthermore, detrended fluctuation analysis (DFA)³⁴ was performed as a measure of the complexity of the VF signal. In the current study, we report on 2 DFA scaling exponents, in small and larger time scales (DFA α 1 and DFA α 2, respectively, Figures S2 and S3).³⁵

Discriminative Models

We used the following stepwise protocol to discriminate between the 2 study groups, using 4 different approaches (Table 1).

Approach 1: Lead II, Single VF Characteristic

In the setting of OHCA, anterolateral direction of the defibrillator paddles is the most standard and recommended method. Therefore, we used ECG information of lead II. First, we assessed the diagnostic performance of an approach using the AMSA of lead II only, to

Table 1. Schematic Description of the Data Analyzing Process

Approach	Recording Direction	VF Waveform Characteristics	Predictor
1	Lead II	AMSA	1 variable
2	Lead II	Entire set of VF characteristics	SVM model with 10 input features* (model A)
3	12 ECG leads	AMSA	SVM model with 23 input features† (model B)
4	12 ECG leads	Entire set of VF characteristics	SVM model with 230 input features‡ (model C)

Four approaches were used to discriminate between patients with and without a myocardial infarction. In approach 1, the AMSA was used as a single variable predictor. Approach 2, 3 and 4 represent SVM discriminative models. Receiver operating characteristic analysis was performed to assess diagnostic accuracy. For approaches 1 and 3, the same procedure as the AMSA was performed for all other individual VF characteristics. AMSA indicates amplitude spectrum area; SVM, support vector machine; and VF, ventricular fibrillation.

*The entire set of 10 VF characteristics, derived from lead II (10×1=10 input features).

†The AMSA derived from all 12 ECG leads (1×12=12 input features) plus the difference of these AMSA values with the AMSA value of lead V1 (1×11 input features), resulting in 23 input features.

‡The entire set of 10 VF characteristics derived from all 12 ECG leads (10×12=120 input features) plus the difference of all VF characteristics with the corresponding VF characteristic of lead V1 (10×11=110 input features), resulting in 230 input features.

discriminate between patients with and without a prior MI. Subsequently, the same procedure was followed for all other individual characteristics of lead II, and we compared their diagnostic yield with that of the AMSA.

Approach 2: Lead II, 10 VF Characteristics (Machine Learning Model A)

To investigate the additional value of more VF features, the entire set of VF waveform characteristics from lead II was used as input for a support vector machine (SVM) classifier, resulting in a model with 10 input features. The SVM process is explained in more detail in Table 1 and Data S2 (Figures S4 and S5). The discriminative ability of the constructed SVM model (model A) was compared with the performance of the prior approach (lead II, AMSA only).

Approach 3: 12 ECG Leads, Single VF Characteristic (Machine Learning Model B)

To investigate the additional value of information from more recording directions, AMSA data of all 12 ECG leads were used as input features for an SVM model. Previous work demonstrated that the VF waveform in lead V1 seems unaffected by the presence or absence of an MI.²⁰ Therefore, we calculated differences with the AMSA of V1 and added these as extra input features, resulting in a model with 23 input features

(Table 1, Data S2). The discriminative performance of this model (model B) was compared with that of the approach with the AMSA of lead II only. The same procedure (ie, lead II versus all leads) was followed for all other individual VF characteristics.

Approach 4: 12 ECG Leads, 10 VF Characteristics (Machine Learning Model C)

To investigate the impact of the input of additional VF characteristics in a 12-lead model, the entire set of 10 VF characteristics from all ECG leads was used, as well as their differences with V1, resulting in an SVM model with 230 input features (Table 1, Data S2). The discriminative performance of this approach (model C) was compared with that of model B.

Ancillary Analyses—Infarct Localization

Previously, we have shown that VF waveform differences associated with underlying etiology are best observed in the ECG leads adjacent to the affected myocardial region.^{20,36} In this context, we performed ancillary analyses to assess the discriminative ability of the SVM models to detect the localization of the prior MI. We used the patient subset with a prior MI and assessed the ability of 2 SVM models, with all VF-waveform characteristics from either lead II or 12 ECG leads. C-statistics were assessed for discrimination between patients with a prior inferior or anterior MI. Patients with involvement of both the anterior and inferior wall were excluded.

Statistical Analysis

Categorical variables were reported as numbers (percentages) and compared between groups using a chi-square test or a Fisher's exact test, whichever was appropriate. Continuous variables were analyzed for Gaussian distribution and reported as means±SDs or medians (interquartile ranges), whichever was appropriate. Comparisons between groups were performed accordingly, with either a Student *t* test or a Mann–Whitney *U* test. Descriptive and comparative statistics were performed with SPSS (Version 25, IBM, Armonk, NY). Receiver operating characteristic analysis was performed to assess the discriminative performances of the models (MedCalc Version 19.1.3, MedCalc Software bv, Ostend, Belgium). C-statistics (95% CI) were compared using the DeLong method.³⁷ Moreover, values of the positive predictive value (PPV) were obtained at the threshold value where Youden's J-statistic ($J = \text{sensitivity} + \text{specificity} - 1$) reaches its maximum, which was considered as the optimal cutoff point of the discriminative model.³⁸ For all statistical analyses, $P < 0.05$ was considered statistically significant. In the case of multiple comparisons, Bonferroni correction was applied.

RESULTS

Study Population

We studied 206 patients with a median age of 64 (57–72) years, of whom 150 were men (73%). Thirty-two percent (67/206) of the implanted ICDs were for secondary prevention, and 32% (66/206) were cardiac resynchronization therapy defibrillator devices. In total, 42% (87/206) of the patients had no evidence of a prior MI. A prior anterior MI was present in 23% (47/206) of the cases, a prior inferior MI was present in 27% (56/206), and 8% (16/206) of the patients had an MI that involved both the inferior and the anterior myocardial wall. Baseline characteristics are reported in Table 2. A representative example of VF induction and termination by an ICD shock is shown in Figure 1.

MI Identification, Lead II

Approach 1, Single VF Characteristic

The AMSA in lead II was lower in patients with than without a prior MI (10.7 mVHz [interquartile range, 8.7–13.4] versus 12.7 mVHz [interquartile range, 9.7–17.7]; $P=0.006$). The discriminative ability of an approach using the AMSA of lead II demonstrated a C-statistic of 0.61 (95% CI, 0.54–0.69), with a PPV of 69% (Table 3).

As for the other individual VF characteristics, we found differences according to the presence or

absence of prior MI, as well as a significant ability to discriminate between the study groups, for the mean absolute amplitude, median slope, organization index, and power spectrum area (Figure 2, blue graphs; Table S1). None of these characteristics had a diagnostic performance that was significantly different from the AMSA.

Approach 2, Entire Set of VF Characteristics

The single-lead SVM model with all 10 VF characteristics of lead II as input features (model A), resulted in a C-statistic of 0.66 (0.59–0.73) with a PPV of 71% at the maximum Youden's J-statistic (Figure 3, Table S2). The discriminative value of this model with the entire set of VF characteristics did not significantly differ from the performance of the approach using only the AMSA in lead II ($P=0.09$; Table 3).

MI Identification, 12 ECG Leads

Approach 3, Single VF Characteristic

The SVM model with the AMSA data of all 12 ECG leads as input features (model B), yielded a C-statistic of 0.75 (95% CI, 0.68–0.81; Figure 3). This was significantly higher than the C-statistic of the approach with the AMSA of lead II only ($P<0.001$; Table 3). The PPV of this model was 77%. None of the other 12-lead SVM models with input from a single VF characteristic

Table 2. Baseline Characteristics of the Study Population

	Cohort of ICD Recipients With VF Waveform Analysis			
	All Patients N=206	Prior MI N=119	No Prior MI N=87	P Value
Medical history				
Age	64 (57–72)	67 (61–75)	59 (48–68)	<0.001
Male sex	150 (73%)	100 (84%)	56 (64%)	0.001
Secondary prevention	67 (33%)	44 (37%)	23 (26%)	0.111
CRT-D	66 (32%)	33 (28%)	33 (38%)	0.121
BMI, kg/m ²	25.9 (23.9–28.9)	26.4 (24.5–29.2)	25.1 (23.0–28.6)	0.034
LVEF, %	34 (27–45)	33 (27–44)	34 (27–46)	0.539
LVIDd index, cm/m ²	3 (2.7–3.3)	3 (2.7–3.3)	3 (2.7–3.3)	0.965
LV mass index, g/m ²	113 (94–134)	111 (96–134)	113 (87–136)	0.635
QRS duration, ms	119 (102–142)	116 (102–138)	122 (102–150)	0.319
Infarct localization				
Anterior infarction	47 (23%)	47 (39%)
Inferior infarction	56 (27%)	56 (47%)
Both	16 (8%)	16 (13%)
Medication				
Beta blocker	185 (90%)	110 (92%)	75 (86%)	0.094
Amiodarone	27 (13%)	18 (15%)	9 (10%)	0.304

BMI indicates body mass index; CRT-D, cardiac resynchronization therapy defibrillator; ICD, implantable cardioverter defibrillator; LV, left ventricular; LVEF, left ventricular ejection fraction; LVIDd, left ventricular internal diastolic diameter; MI, myocardial infarction; and VF, ventricular fibrillation.

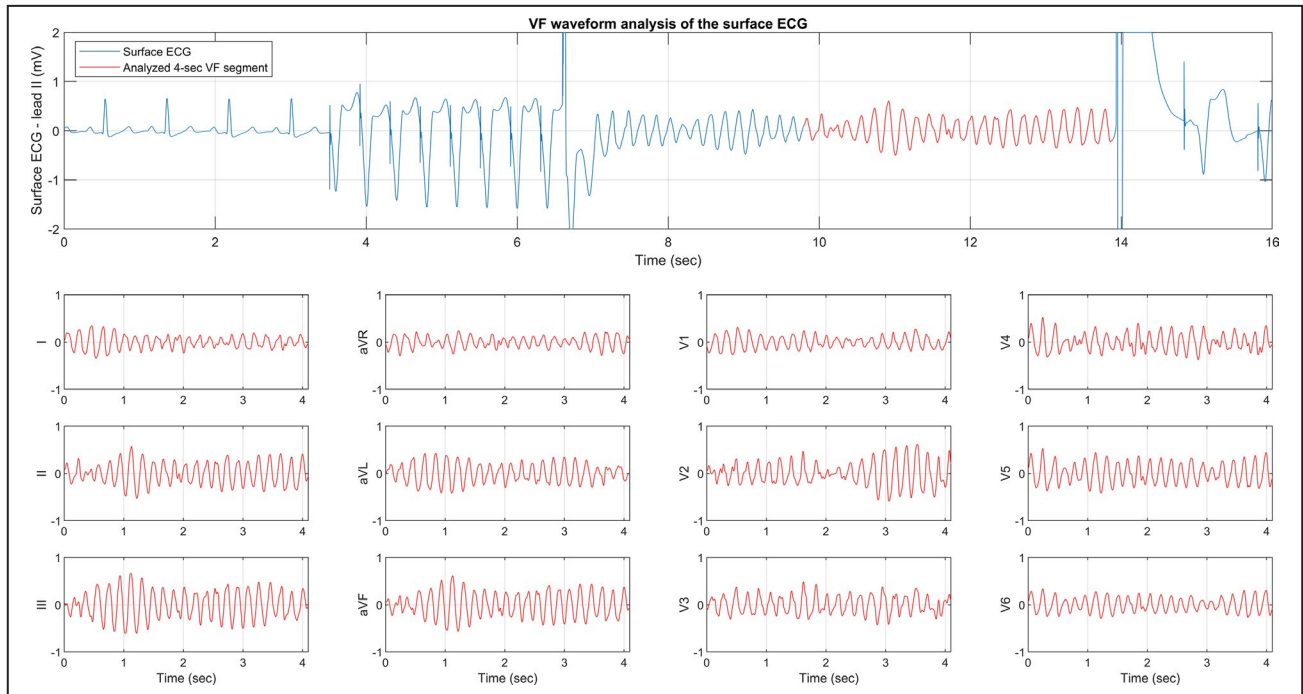


Figure 1. The VF waveform during defibrillation testing after ICD implantation.

In this representative example, the ECG of a single ECG lead (lead II) is presented (upper plot). After initial pacing, VF is induced by a shock on the T wave. VF is recognized by the ICD and terminated by a defibrillatory shock. The red selection (4.1 seconds, 12-lead subplot) is used for VF waveform analysis. ICD indicates implantable cardioverter defibrillator; and VF, ventricular fibrillation.

demonstrated a significantly better diagnostic performance than the approach of using the AMSA data of all 12 ECG leads. The performance of the 12-lead AMSA model was superior to those that contained 12-lead information of the bandwidth, DFA α 1, and DFA α 2 (Figure 2, red graphs; Table S3).

Approach 4, Entire Set of VF Characteristics

The 12-lead SVM model, with information of all VF characteristics from all 12 ECG leads (model C) demonstrated a C-statistic of 0.74 (95% CI, 0.67–0.80) with a PPV of 71% (Figure 3, Table S2). The discriminative ability was not significantly different compared with the performance of model B ($P=0.66$; Table 3).

Table 3. Results of the Primary Analyses

Approach	SVM Model	C-Statistic*	Positive Predictive Value, %
1) lead II, AMSA only	...	0.61 (0.54–0.69)	69
2) lead II, all VF characteristics	A	0.66 (0.59–0.73) [†]	71
3) 12 leads, AMSA only	B	0.75 (0.68–0.81) [‡]	77
4) 12 leads, all VF characteristics	C	0.74 (0.67–0.80) [§]	71

Model performances of the different approaches are presented by the area under the receiver operating characteristic curve (C-statistic). The positive predictive value is obtained at the threshold value where Youden’s J-statistic ($J = \text{sensitivity} + \text{specificity} - 1$) reaches its maximum. AMSA indicates amplitude spectrum area; SVM, support vector machine; and VF, ventricular fibrillation.

* $P < 0.017$ was considered statistically significant after Bonferroni correction.

[†]Nonsignificant ($P = 0.09$) compared with approach 1.

[‡]Significantly different ($P < 0.001$) compared with approach 1.

[§]Nonsignificant ($P = 0.66$) compared with approach 3.

Infarct Localization

In total, 39% (47/119) of the patients with MI had a prior anterior MI and 47% (56/119) a prior inferior MI. An SVM model with all VF waveform characteristics of lead II demonstrated a C-statistic of 0.77 (95% CI, 0.67–0.85) for identification of the infarcted area, with a PPV of 74% for detection of an inferior MI. A machine learning model combining all VF waveform characteristics from 12 ECG leads demonstrated a C-statistic of 0.89 (95% CI, 0.81–0.94) and a PPV of 83% for identification of an inferior MI (P for comparison = 0.01; Figure S6).

DISCUSSION

In follow-up on studies that showed associations between the VF waveform and underlying etiology,

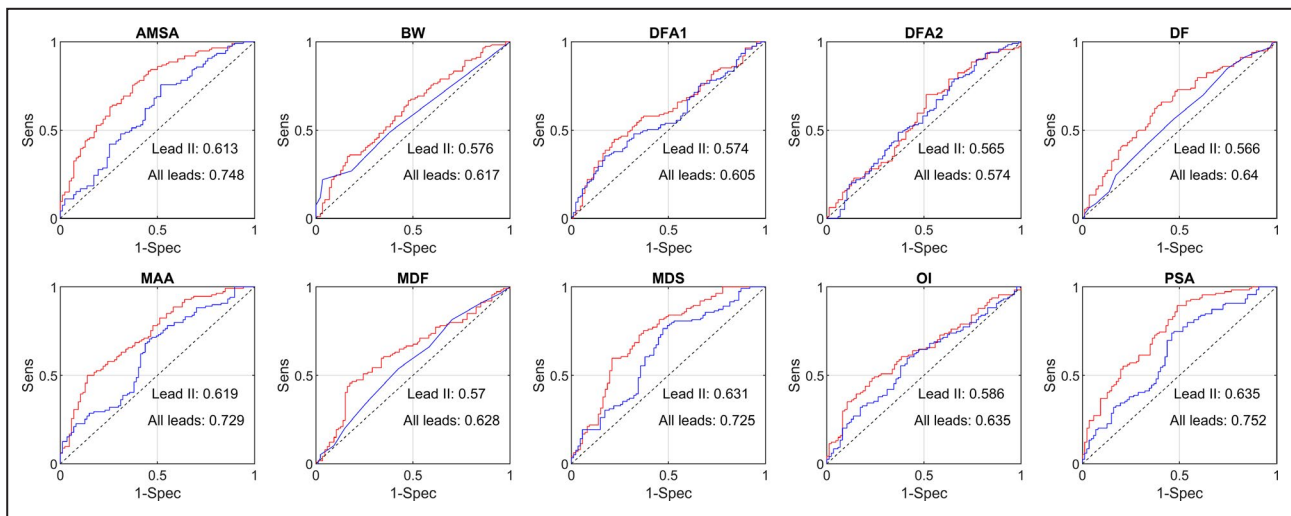


Figure 2. Discriminative ability of all individual VF waveform characteristics.

Receiver operating characteristic curves of individual VF waveform characteristics of a single lead (lead II, blue) and from SVM models using that specific VF characteristic of all 12 ECG leads (red). AMSA indicates amplitude spectrum area; BW, bandwidth; DF, dominant frequency; DFA, detrended fluctuation analysis; MAA, mean absolute amplitude; MDF, median frequency; MDS, median slope; MI, myocardial infarction; OI, organization index; PSA, power spectrum analysis; Sens, sensitivity; Spec, specificity; SVM, support vector machine; and VF, ventricular fibrillation.

we now present the first study in humans with focus on diagnostic performance, and demonstrate that computerized VF waveform analysis may have the potential to actually detect an MI using a single ECG lead (lead II). Data from diagnostic machine learning approaches showed that additional input from a combination of VF characteristics rather than from a single VF feature did not improve discriminative ability, whereas input from all 12 ECG leads resulted in a significantly higher diagnostic accuracy. These findings warrant additional confirmative experimental studies. Appreciating that VF morphology may be even more affected in case of acute MIs,^{16–18} our findings on prior MI can be considered as pilot data for future in-field initiatives to study the diagnostic performance of an acute MI, which could pave the way toward very early triage and treatment of patients with cardiac arrest.

The VF Waveform and Cardiac Arrest

Over the years, analysis of the VF waveform has become a new instrument in cardiac arrest research, as it is easily obtainable, with the potential to provide information in the very early, prehospital phase of resuscitation.^{3,39,40} The AMSA is the key characteristic of interest in most studies and has been shown to reflect myocardial metabolic state.⁴¹ Several studies have demonstrated associations between the AMSA and cardiac arrest outcomes (defibrillation success, neurologic survival).^{4,42,43} In follow-up, the first initiatives to study the predictive value of the VF waveform have been published, with promising results using machine

learning approaches with input of a wide variety of VF characteristics.^{3–6} As a next step, a randomized trial has been initiated to investigate defibrillation success with a standard cardiopulmonary resuscitation protocol, compared with a protocol with a smart defibrillator that provides real-time AMSA analysis and guides defibrillation timing.⁷

Another potential application of VF waveform analysis could be detection of underlying heart disease, such as an MI. Infarct model studies have shown markedly different VF waveform characteristics in the case of a prior MI, with even more pronounced changes during acute coronary occlusion. More specifically, these animal studies demonstrated that ischemia results in VF waveform changes early after initiation of VF and that differences between prior and acute MI seem to increase with longer arrest duration.^{14–16} As of yet, human studies have been contradictory. While retrospective cohort studies in patients with OHCA with ST-segment-elevation MI have reported associations with lower AMSA values,^{17,18} others did not observe significant VF waveform differences between patients with ST-segment-elevation MI, non-ST-segment-elevation MI and nonischemic OHCA.⁴⁴

In follow-up on previous studies describing associations, and as a first step toward potential future studies on acute MI identification, we performed this experimental study on the diagnostic ability of VF waveform analysis to detect a prior MI. From an electrophysiological perspective, this study adds to the current knowledge that computerized VF-waveform analysis may allow for identification of underlying

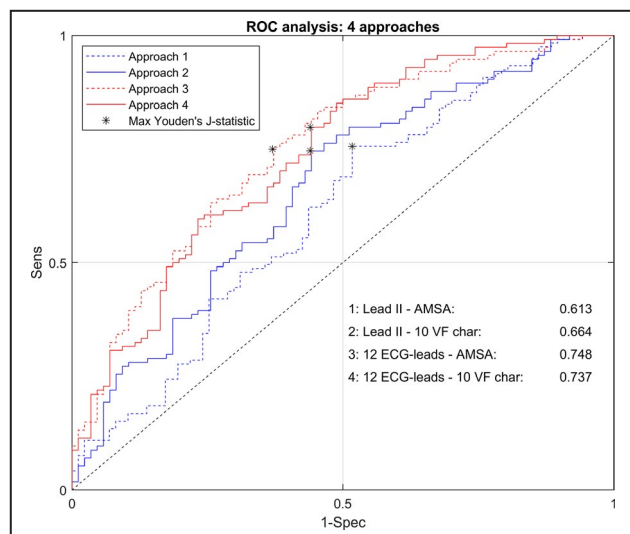


Figure 3. Identification of an MI, 4 different approaches. ROC curves for MI identification, using either the AMSA of a single lead (lead II, approach 1, blue dashed line), an SVM model with combined VF characteristics of lead II (approach 2, blue solid line), an SVM model with the AMSA of all 12 ECG leads (approach 3, red dashed line) or an SVM model with combined VF characteristics of all 12 ECG leads (approach 4, red solid line). The positive predictive value is obtained at the threshold value where Youden's J-statistic ($J = \text{sensitivity} + \text{specificity} - 1$) reaches its maximum. AMSA indicates amplitude spectrum area; char, characteristics; MI, myocardial infarction; ROC, receiver operating characteristic; Sens, sensitivity; Spec, specificity; SVM, support vector machine; and VF, ventricular fibrillation.

disease, in this case a prior MI. Our current findings can be considered as pilot data for OHCA studies on acute MI.

Detection of MI Using the VF Waveform

Initially, we studied the diagnostic performance using VF waveform information from lead II, as a proxy for the paddle ECG. We demonstrated that with the AMSA of lead II only, it was feasible to detect a prior MI. Discriminative performance was moderate, without significant improvement when using a combination of VF characteristics rather than a single VF feature. With use of input from all 12 ECG leads, the diagnostic accuracy significantly improved as compared with the single-lead approach, again without additional yield from a combination of VF characteristics.

Our observations that machine learning techniques with combined information from multiple ECG leads resulted in markedly improved discriminative performances is in line with previous studies that showed importance of the recording direction of VF.^{20,45} In previous work, we observed differences in VF waveform characteristics in patients with and without a prior MI, especially in the leads adjacent to the infarcted area.²⁰ These differences were not present in lead V1. As

such, lead V1 may serve as a reference electrode for each patient individually. This is the rationale behind the additional input feature that consists of the assessment of VF waveform differences between each of the respective ECG leads with V1.

Building on the hypothesis that infarcted myocardium results in regional VF waveform differences, we performed ancillary analyses on the subset with either anterior or inferior MI to determine the diagnostic accuracy in terms of infarct localization. Machine learning models combining information from 12 ECG leads were very accurate in the identification of the infarcted area (C-statistic, 0.89), which was superior to a single-lead approach (C-statistic, 0.77). In short, these collective findings support the concept of regional ECG differences in VF characteristics in patients with MI. Appreciating that VF waveform changes have been reported to be more apparent in acute than in prior MI, this paves the way for future work on the detection of acute MI with use of computerized VF waveform analysis.

Implications

Our observation that identification of a prior MI is feasible with computerized analysis of the VF waveform provides impetus for further experimental and clinical studies. Given the challenging conditions of in-field cardiac arrest research, additional work is needed before undertaking an out-of-hospital study with a smart defibrillator, aiming at detection of acute MI with VF waveform analysis.

Experimental studies will have to focus on further exploration and optimization of the SVM models (in terms of tuning parameters and input features) with primary focus on an approach using a single lead (II), as this most closely reflects current daily practice with defibrillator pads. From a scientific point of view, more data are needed on the optimal number and positions of the ECG electrodes, as well as on quantification of the potential additional diagnostic yield of these options.

In terms of clinical studies, prospective cardiac arrest registries with systematically collected ECG data and coronary angiography information could help answer whether VF waveform information from the paddle ECG can contribute to identification of an acute MI. Potentially, a smart defibrillator with a VF waveform-based algorithm may help to identify patients with an acute MI in a much earlier stage of cardiac arrest. As of yet, the diagnosis of acute MI is restricted to those patients who (eventually) achieve return of spontaneous circulation. Especially in patients with refractory VF, there is a high burden of coronary artery disease.^{9,10} Identification of acute MI as an underlying, treatable cause of cardiac arrest

would be a first step toward research on more individualized resuscitation strategies. In an era of upcoming treatment options like transport with mechanical resuscitation and extracorporeal membrane oxygenation, a smart defibrillator may provide important benefits on shock success, prognosis, and possibly the underlying cause to guide triage and decision making.^{3,10,11,40,46}

Limitations

In this experimental setting, we investigated induced, short-duration VF, which has previously been reported to be more organized than in-field VF.^{47,48} Moreover, the current rhythm recordings reflect early VF, in an earlier stage than observed during OHCA. This may limit generalizability to VF in the OHCA setting. Appreciating the logistic challenge of a prospective in-field study with VF waveform analysis, we opted to first investigate the feasibility of detecting underlying etiology under controlled conditions, including multiple ECG leads. During cardiac arrest, the appearance of the VF waveform develops over time, and morphology also depends on the quality of administered cardiopulmonary resuscitation, factors that were not addressed in this experimental model but could contribute to improve discriminative ability in the field.^{43,49,50}

Finally, despite the fact that we report on the largest VF cohort to date with 12-lead ECG recordings, the amount of input features is relatively small for machine learning purposes. In this context, future studies with larger data sets may provide valuable insights.

CONCLUSIONS

This proof-of-concept study provides the first evidence that computerized VF waveform analysis allows for actual detection of a prior MI. During ongoing VF, MI identification is modestly feasible with use of the AMSA of lead II. Machine learning approaches suggest that information from multiple ECG recording directions rather than input of multiple VF characteristics results in superior discriminative performances. Appreciating that previous studies have indicated that VF waveform changes are even more pronounced in acute MI, our findings fuel the concept that VF analysis may contribute to the detection of an acute MI. This calls for additional studies that may ultimately pave the way toward more individualized cardiac arrest care with assistance of a “smart defibrillator.”

ARTICLE INFORMATION

Received March 28, 2020; accepted August 31, 2020.

Affiliations

From the Department of Cardiology, Radboud University Medical Center, Nijmegen, The Netherlands.

Acknowledgments

The authors thank H.J. Zwart, PhD, and G. Meinsma, PhD (Faculty of Electrical Engineering, Mathematics & Computer Science, University of Twente, Enschede, The Netherlands), for their support with regard to the technical analysis on the VF waveform and construction of the SVM models. Moreover, we sincerely acknowledge S.D. Verboom, BSc, and K.M. van der Sluijs, BSc (University of Twente, Enschede, The Netherlands), for their valuable input and critical revision of the article. Finally, we thank Dr P. Vart (Department of Health Evidence, Radboud University Medical Center, Nijmegen, the Netherlands) for his expertise on the statistical analyses.

Sources of Funding

None.

Disclosures

Dr Van Royen received research grants from Abbott, Biotronik, AstraZeneca, and Philips and professional fees from Abbott and Medtronic. The remaining authors have no disclosures to report.

Supplementary Materials

Data S1–S2

Tables S1–S3

Figures S1–S6

REFERENCES

- Berdowski J, Berg RA, Tijssen JG, Koster RW. Global incidences of out-of-hospital cardiac arrest and survival rates: systematic review of 67 prospective studies. *Resuscitation*. 2010;81:1479–1487.
- Daya MR, Schmicker RH, Zive DM, Rea TD, Nichol G, Buick JE, Brooks S, Christenson J, MacPhee R, Craig A, et al. Out-of-hospital cardiac arrest survival improving over time: results from the Resuscitation Outcomes Consortium (ROC). *Resuscitation*. 2015;91:108–115.
- Ristagno G, Mauri T, Cesana G, Li Y, Finzi A, Fumagalli F, Rossi G, Grieco N, Migliori M, Andreassi A, et al. Amplitude spectrum area to guide defibrillation: a validation on 1617 patients with ventricular fibrillation. *Circulation*. 2015;131:478–487.
- Indik JH, Conover Z, McGovern M, Silver AE, Spaite DW, Bobrow BJ, Kern KB. Amplitude-spectral area and chest compression release velocity independently predict hospital discharge and good neurological outcome in ventricular fibrillation out-of-hospital cardiac arrest. *Resuscitation*. 2015;92:122–128.
- Howe A, Escalona OJ, Di Maio R, Massot B, Cromie NA, Darragh KM, Adgey J, McEaney DJ. A support vector machine for predicting defibrillation outcomes from waveform metrics. *Resuscitation*. 2014;85:343–349.
- Coult J, Blackwood J, Sherman L, Rea TD, Kudenchuk PJ, Kwok H. Ventricular fibrillation waveform analysis during chest compressions to predict survival from cardiac arrest. *Circ Arrhythm Electrophysiol*. 2019;12:e006924. DOI: 10.1161/CIRCEP.118.006924.
- Ristagno G, Latini R. Real time amplitude spectrum area to guide defibrillation. [Internet]. Identifier: NCT03237910; 2017 Aug 3. Available at: [ClinicalTrials.gov/https://ClinicalTrials.gov/show/NCT03237910](https://ClinicalTrials.gov/show/NCT03237910). Accessed August 12, 2020.
- Link MS, Berkow LC, Kudenchuk PJ, Halperin HR, Hess EP, Moitra VK, Neumar RW, O’Neil BJ, Paxton JH, Silvers SM, et al. Part 7: adult advanced cardiovascular life support: 2015 American Heart Association Guidelines Update for Cardiopulmonary Resuscitation and Emergency Cardiovascular Care. *Circulation*. 2015;132:S444–S464.
- Spaulding CM, Joly LM, Rosenberg A, Monchi M, Weber SN, Dhainaut JF, Carli P. Immediate coronary angiography in survivors of out-of-hospital cardiac arrest. *N Engl J Med*. 1997;336:1629–1633.
- Yannopoulos D, Bartos JA, Raveendran G, Conterato M, Frascione RJ, Trembley A, John R, Connert J, Benditt DG, Lurie KG, et al. Coronary artery disease in patients with out-of-hospital refractory ventricular fibrillation cardiac arrest. *J Am Coll Cardiol*. 2017;70:1109–1117.
- Dumas F, Cariou A, Manzo-Silberman S, Grimaldi D, Vivien B, Rosencher J, Empana JP, Carli P, Mira JP, Jouven X, et al. Immediate percutaneous coronary intervention is associated with better survival

- after out-of-hospital cardiac arrest: insights from the PROCAT (Parisian Region Out of hospital Cardiac Arrest) registry. *Circ Cardiovasc Interv.* 2010;3:200–207.
12. Dumas F, Manzo-Silberman S, Fichet J, Mami Z, Zuber B, Vivien B, Chenevier-Gobeaux C, Varenne O, Empana JP, Pene F, et al. Can early cardiac troponin I measurement help to predict recent coronary occlusion in out-of-hospital cardiac arrest survivors? *Crit Care Med.* 2012;40:1777–1784.
 13. Coppler PJ, Dezfulian C. The quest continues to identify coronary occlusion in OHCA without ST elevation. *Resuscitation.* 2020;146:258–260.
 14. Sherman LD, Niemann JT, Rosborough JP, Menegazzi JJ. The effect of ischemia on ventricular fibrillation as measured by fractal dimension and frequency measures. *Resuscitation.* 2007;75:499–505.
 15. Indik JH, Donnerstein RL, Hilwig RW, Zuercher M, Feigelman J, Kern KB, Berg MD, Berg RA. The influence of myocardial substrate on ventricular fibrillation waveform: a swine model of acute and postmyocardial infarction. *Crit Care Med.* 2008;36:2136–2142.
 16. Indik JH, Allen D, Gura M, Dameff C, Hilwig RW, Kern KB. Utility of the ventricular fibrillation waveform to predict a return of spontaneous circulation and distinguish acute from post myocardial infarction or normal swine in ventricular fibrillation cardiac arrest. *Circ Arrhythm Electrophysiol.* 2011;4:337–343.
 17. Olasveengen TM, Eftestol T, Gundersen K, Wik L, Sunde K. Acute ischemic heart disease alters ventricular fibrillation waveform characteristics in out-of-hospital cardiac arrest. *Resuscitation.* 2009;80:412–417.
 18. Hulleman M, Salcido DD, Menegazzi JJ, Souverein PC, Tan HL, Blom MT, Koster RW. Predictive value of amplitude spectrum area of ventricular fibrillation waveform in patients with acute or previous myocardial infarction in out-of-hospital cardiac arrest. *Resuscitation.* 2017;120:125–131.
 19. Bonnes JL, Keuper W, Westra SW, Zegers ES, Oostendorp TF, Brouwer MA, Smeets JL. Characteristics of ventricular fibrillation in relation to cardiac aetiology and shock success: a waveform analysis study in ICD-patients. *Resuscitation.* 2015;86:95–99.
 20. Bonnes JL, Thannhauser J, Hermans MC, Westra SW, Oostendorp TF, Meinsma G, de Boer MJ, Brouwer MA, Smeets JL. Ventricular fibrillation waveform characteristics differ according to the presence of a previous myocardial infarction: a surface ECG study in ICD-patients. *Resuscitation.* 2015;96:239–245.
 21. Gundersen K, Kvaløy JT, Kramer-Johansen J, Steen PA, Eftestøl T. Development of the probability of return of spontaneous circulation in intervals without chest compressions during out-of-hospital cardiac arrest: an observational study. *BMC Med.* 2009;7:6.
 22. Gazmuri RJ, Kaufman CL, Baetiong A, Radhakrishnan J. Ventricular fibrillation waveform changes during controlled coronary perfusion using extracorporeal circulation in a swine model. *PLoS One.* 2016;11:e0161166.
 23. Indik JH, Hilwig RW, Zuercher M, Kern KB, Berg MD, Berg RA. Pre-shock cardiopulmonary resuscitation worsens outcome from circulatory phase ventricular fibrillation with acute coronary artery obstruction in swine. *Circ Arrhythm Electrophysiol.* 2009;2:179–184.
 24. Thygesen K, Alpert JS, Jaffe AS, Simoons ML, Chaitman BR, White HD, Thygesen K, Alpert JS, White HD, Jaffe AS, et al. Third universal definition of myocardial infarction. *Eur Heart J.* 2012;33:2551–2567.
 25. Zimetbaum PJ, Josephson ME. Use of the electrocardiogram in acute myocardial infarction. *N Engl J Med.* 2003;348:933–940.
 26. Zipes DP, Camm AJ, Borggrefe M, Buxton AE, Chaitman B, Fromer M, Gregoratos G, Klein G, Moss AJ, Myerburg RJ, et al. ACC/AHA/ESC 2006 guidelines for management of patients with ventricular arrhythmias and the prevention of sudden cardiac death: a report of the American College of Cardiology/American Heart Association Task Force and the European Society of Cardiology Committee for Practice Guidelines (writing committee to develop Guidelines for Management of Patients With Ventricular Arrhythmias and the Prevention of Sudden Cardiac Death): developed in collaboration with the European Heart Rhythm Association and the Heart Rhythm Society. *Circulation.* 2006;114:e385–e484.
 27. Weaver WD, Cobb LA, Dennis D, Ray R, Hallstrom AP, Copass MK. Amplitude of ventricular fibrillation waveform and outcome after cardiac arrest. *Ann Intern Med.* 1985;102:53–55.
 28. Neurauber A, Eftestol T, Kramer-Johansen J, Abella BS, Sunde K, Wenzel V, Lindner KH, Eilevstjonn J, Mykebust H, Steen PA, et al. Prediction of countershock success using single features from multiple ventricular fibrillation frequency bands and feature combinations using neural networks. *Resuscitation.* 2007;73:253–263.
 29. Povoas HP, Bisera J. Electrocardiographic waveform analysis for predicting the success of defibrillation. *Crit Care Med.* 2000;28:N210–N211.
 30. Carlisle EJ, Allen JD, Kernohan WG, Anderson J, Adgey AA. Fourier analysis of ventricular fibrillation of varied aetiology. *Eur Heart J.* 1990;11:173–181.
 31. Brown CG, Dzwonczyk R, Werman HA, Hamlin RL. Estimating the duration of ventricular fibrillation. *Ann Emerg Med.* 1989;18:1181–1185.
 32. Indik JH, Donnerstein RL, Kern KB, Goldman S, Gaballa MA, Berg RA. Ventricular fibrillation waveform characteristics are different in ischemic heart failure compared with structurally normal hearts. *Resuscitation.* 2006;69:471–477.
 33. Sanchez-Munoz JJ, Rojo-Alvarez JL, Garcia-Alberola A, Everss E, Requena-Carrion J, Ortiz M, Alonso-Atienza F, Valdes-Chavarri M. Effects of the location of myocardial infarction on the spectral characteristics of ventricular fibrillation. *Pacing Clin Electrophysiol.* 2008;31:660–665.
 34. Peng CK, Havlin S, Stanley HE, Goldberger AL. Quantification of scaling exponents and crossover phenomena in nonstationary heartbeat time series. *Chaos.* 1995;5:82–87.
 35. Lin LY, Lo MT, Ko PC, Lin C, Chiang WC, Liu YB, Hu K, Lin JL, Chen WJ, Ma MH. Detrended fluctuation analysis predicts successful defibrillation for out-of-hospital ventricular fibrillation cardiac arrest. *Resuscitation.* 2010;81:297–301.
 36. Bonnes JL, Thannhauser J, Nas J, Westra SW, Jansen RMG, Meinsma G, de Boer MJ, Smeets J, Keuper W, Brouwer MA. Ventricular fibrillation waveform characteristics of the surface ECG: impact of the left ventricular diameter and mass. *Resuscitation.* 2017;115:82–89.
 37. DeLong ER, DeLong DM, Clarke-Pearson DL. Comparing the areas under two or more correlated receiver operating characteristic curves: a nonparametric approach. *Biometrics.* 1988;44:837–845.
 38. Youden WJ. Index for rating diagnostic tests. *Cancer.* 1950;3:32–35.
 39. Reed MJ, Clegg GR, Robertson CE. Analysing the ventricular fibrillation waveform. *Resuscitation.* 2003;57:11–20.
 40. Indik JH, Conover Z, McGovern M, Silver AE, Spaitte DW, Bobrow BJ, Kern KB. Association of amplitude spectral area of the ventricular fibrillation waveform with survival of out-of-hospital ventricular fibrillation cardiac arrest. *J Am Coll Cardiol.* 2014;64:1362–1369.
 41. Salcido DD, Menegazzi JJ, Suffoletto BP, Logue ES, Sherman LD. Association of intramyocardial high energy phosphate concentrations with quantitative measures of the ventricular fibrillation electrocardiogram waveform. *Resuscitation.* 2009;80:946–950.
 42. Young C, Bisera J, Gehman S, Snyder D, Tang W, Weil MH. Amplitude spectrum area: measuring the probability of successful defibrillation as applied to human data. *Crit Care Med.* 2004;32:S356–S358.
 43. Schoene P, Coult J, Murphy L, Fahrenbruch C, Blackwood J, Kudenchuk P, Sherman L, Rea T. Course of quantitative ventricular fibrillation waveform measure and outcome following out-of-hospital cardiac arrest. *Heart Rhythm.* 2014;11:230–236.
 44. Hidano D, Coult J, Blackwood J, Fahrenbruch C, Kwok H, Kudenchuk P, Rea T. Ventricular fibrillation waveform measures and the etiology of cardiac arrest. *Resuscitation.* 2016;109:71–75.
 45. Indik JH, Peters CM, Donnerstein RL, Ott P, Kern KB, Berg RA. Direction of signal recording affects waveform characteristics of ventricular fibrillation in humans undergoing defibrillation testing during ICD implantation. *Resuscitation.* 2008;78:38–45.
 46. Bougouin W, Dumas F, Lamhaut L, Marijon E, Carli P, Combes A, Pirracchio R, Aissaoui N, Karam N, Deye N, et al. Extracorporeal cardiopulmonary resuscitation in out-of-hospital cardiac arrest: a registry study. *Eur Heart J.* 2020;41:1961–1971.
 47. Sanchez-Munoz JJ, Rojo-Alvarez JL, Garcia-Alberola A, Everss E, Alonso-Atienza F, Ortiz M, Martinez-Sanchez J, Ramos-Lopez J, Valdes-Chavarri M. Spectral analysis of intracardiac electrograms during induced and spontaneous ventricular fibrillation in humans. *Europace.* 2009;11:328–331.
 48. Lever NA, Newall EG, Larsen PD. Differences in the characteristics of induced and spontaneous episodes of ventricular fibrillation. *Europace.* 2007;9:1054–1058.
 49. Thannhauser J, Nas J, van Grunsven PM, Meinsma G, Zwart HJ, de Boer MJ, van Royen N, Bonnes JL, Brouwer MA. The ventricular fibrillation waveform in relation to shock success in early vs. late phases of out-of-hospital resuscitation. *Resuscitation.* 2019;139:99–105.
 50. Eftestol T, Wik L, Sunde K, Steen PA. Effects of cardiopulmonary resuscitation on predictors of ventricular fibrillation defibrillation success during out-of-hospital cardiac arrest. *Circulation.* 2004;110:10–15.

SUPPLEMENTAL MATERIAL

Data S1.

Supplemental Methods 1. Calculation of VF-waveform characteristics

Data pre-processing

Each ventricular fibrillation (VF) signal was sampled at a sampling frequency of $f_s = 1000$ Hz. The characteristics were determined from the time segment of 4.1 seconds prior to the first shock delivery. Each segment was pre-processed with a fourth-order Butterworth bandpass filter with cut-off frequencies of 1 and 48 Hz. To cancel phase shift the filter was applied once forward and once backward in time, which is what the Matlab command *filtfilt* does, resulting in the filtered VF-segment x_n , for which $n \in \{1, 2, \dots, N\}$ with number of samples of $N = 4096$.

Time domain parameters

- The *mean absolute amplitude* (mV) is computed as the mean of all absolute samples of the filtered time segment, following:

$$MAA = \frac{1}{N} \sum_{i=1}^N |x_i|$$

- The *median slope* (mVs⁻¹) is calculated by taking the median of all sample-to-sample differences in the signal, following:

$$MDS = \text{median}(|x_i - x_{i-1}| \cdot f_s)$$

for samples $2 \leq i \leq 4096$.

Frequency domain parameters

A standard Fast Fourier Transform (FFT) of the VF segment returns N Fourier coefficients $\hat{x}_1, \hat{x}_2, \dots, \hat{x}_N$. Only the first $N/2$ coefficients are relevant and they correspond to the $N/2$ frequencies $f_k = k \cdot f_s/N$ with $k \in \{0, 1, \dots, N/2\}$.

- The *amplitude spectrum area* (mVHz) is defined as

$$AMSA = \frac{2}{N} \sum_{k=0}^{N/2} |\hat{x}_k \cdot f_k|,$$

but in this sum only those indices k are taken into account for which $2 \leq f_k \leq 48$.

The power spectrum of the VF signal, also called the power spectral density, describes the power present in the signal as a function of the frequency, per unit frequency. It is defined as

$$PSD_k = \beta_k |\hat{x}_k|^2, \text{ with } k \in \{0, 1, \dots, N/2\} \text{ and } \beta_k = \begin{cases} 2 \frac{1}{f_s N} & k \in \{1, 2, \dots, \frac{N}{2} - 1\} \\ \frac{1}{f_s N} & k = 0 \text{ or } k = N/2 \end{cases}$$

- From the power spectrum, the *power spectrum area* (mV²Hz) was calculated as:

$$PSA = \frac{f_s}{N} \sum_{k=0}^{N/2} |PSD_k \cdot f_k|$$

- The *dominant frequency* (Hz) is defined as the frequency f_k for which PSD_k attains his maximum:

$$DF = \arg \max_k PSD_k$$

- The *median frequency* (Hz) is computed as the smallest frequency f_k for which the trapezoidal integral approximation $(\sum_{i=0}^k |\hat{x}_i|^2) - (|\hat{x}_0|^2 + |\hat{x}_k|^2)/2$ is at least 50% of the total trapezoidal $(\sum_{i=0}^{N/2} |\hat{x}_i|^2) - (|\hat{x}_0|^2 + |\hat{x}_{N/2}|^2)/2$. Likewise, we compute the 25% and 75% frequencies and then the *bandwidth* (Hz) is defined as the difference between these two frequencies.

Measures of signal organization

Organization index

First, the bandwidth of the fundamental peak (corresponding to the dominant frequency) was obtained, given by a 75% amplitude decrease. Subsequently, harmonic peaks corresponding to the DF were assessed, as well as the bandwidth of these harmonic peaks.

- The *organization index* was defined as the ratio between the summed power of the bandwidth of the fundamental and its harmonic peaks, and the total power (Figure S1).

Detrended fluctuation analysis

Detrended fluctuation analysis (DFA) gives information about the complexity of the VF morphology. DFA-measures are computed following standardized steps, which is visualized in Figure S2.

Correction for the offset of the original time series by subtracting the mean of the signal (1); The resulting signal is subsequently integrated by taking the cumulative sum of the signal (2); This signal is divided in boxes of equal sample length n , with $n \in \{2^1, 2^2 \dots 2^{12} = 4096\}$. In each box, the local linear trend is calculated (3) and subtracted from the integrated time series (4). From these detrended signals, the root mean square (RMS) is calculated, representing the fluctuation F in that specific box size. This process is repeated for all values of n ; (5) the relationship between $F(n)$ and n is plotted on logarithmic axes. The DFA scaling exponent α is the slope of the trend line of this function, estimated using linear regression.

In the current study, we report on two DFA scaling exponents (Figure S3):

- $DFA\alpha_1$: defined as the DFA scaling exponent on small time scales, i.e. 0.004 to 0.128 seconds.
- $DFA\alpha_2$: defined as the DFA scaling exponent on larger time scales, i.e. 0.128 to 4.0 seconds.

Data S2. Support vector machine

Support vector machine (SVM) is a machine learning technique which enables discrimination between two classes by an algorithm that maximizes the distance between these classes, using a prespecified amount of *input features*. The mathematical function that gives the optimal separation between the classes is called the *hyperplane*, which allows for discrimination between the two classes. SVMs have been used in multiple VF-studies to combine VF-waveform characteristics and predict defibrillation success and clinical outcome measures. [5,6]

Settings of SVM-models in this study

In the current study, the function *fitsvm* in Matlab (version 2018a, The Mathworks, Natick, USA) was used for training and validation of the SVM-models. In these preliminary analyses to investigate the concept of machine learning for MI-identification, fixed settings were used for model optimization. Models were trained using normalized input features (mean = 0, standard deviation = 1). Optimization of the regularization parameter C was performed by varying this parameter following: $C = 2^{-7}, 2^{-6} \dots 2^7$ and taking the value with the maximum AUC (Figure S4). For all models, a linear kernel was used, with automatic scaling of the kernel. Five-fold cross validation was performed using the *crossval* function in Matlab. The process of data analysis is visualized in Figure S5.

Data flowchart and input features

The input *feature matrix* consists of $N \times M$ elements, with N the number of patients and M the number of input features. M is determined by the number of leads (either a single lead or 12-leads) and the number of VF-characteristics per lead (either a single lead or the entire set of 10 VF-characteristics). In case of a 12-lead approach, the difference with V1 was calculated for each VF-characteristic as well. Hence, M differed for all three SVM-approaches that were used:

(A) Single lead II, 10 VF-waveform characteristics (1 lead x 10 VF-characteristics =
10 input features per patient

(B) 12 leads, single VF-characteristics (12 leads x 1 VF-characteristic + 11 x 1 difference with
V1 = 23 input features

(C) 12 leads, 10 VF-characteristics (12 leads x 10 VF-characteristic + 11 x 10 difference with V1
= 230 input features

Table S1. Individual VF-characteristics and discriminative performances, single lead II.

VF-characteristic	All patients N=206	MI +	MI -	P-value comparison	C-statistic
AMSA	11.3 (9.1-16.1)	10.7 (8.7-13.4)	12.7 (9.7-17.7)	0.006	0.613 (0.535-0.692)
BW	.49 (.49-.73)	.49 (.49-.98)	.49 (.24-.73)	0.06	0.576 (0.498-0.653) §
DFA1	1.97 (1.95-1.98)	1.96 (1.95-1.98)	1.97 (1.96-1.98)	0.07	0.574 (0.496-0.652) §
DFA2	.26 (.22-.31)	.27 (.23-.31)	.25 (.21-.30)	0.11	0.565 (0.485-0.646) §
DF	5.1 (4.9-5.6)	5.1 (4.9-5.6)	5.4 (4.9-5.9)	0.11	0.566 (0.486-0.650) §
MAA	.15 (.11-.24)	.14 (.10-.21)	.19 (.12-.27)	0.003	0.619 (0.541-0.697) §
MDF	5.4 (4.9-5.6)	5.1 (4.9-5.6)	5.4 (4.9-5.9)	0.08	0.570 (0.491-0.649) §
MDS	4.6 (3.5-7.1)	4.2 (3.2-5.7)	6.1 (3.8-8.0)	0.001	0.631 (0.553-0.709) §
OI	.70 (.56-.78)	.68 (.51-.77)	.72 (.60-.79)	0.04	0.586 (0.508-0.664) §
PSA	.18 (.10-.42)	.17 (.08-.27)	.26 (.12-.58)	0.001	0.625 (0.558-0.713) §

§ Statistically not different from the C-statistic of AMSA (De Long method $p > 0.006$ after Bonferroni correction)

Table S2. Performances and characteristics of SVM-models with combined VF-characteristics.

SVM-model	C-statistic	Optimal regularization parameter C
Lead II	0.66 (0.59-0.73)	2^3
12 leads	0.74 (0.67-0.80)	2^{-2}

Table S3. Individual characteristics and model performances, 12-lead SVM-models.

SVM-model	C-statistic	Optimal regularization parameter C
AMSA, 12-leads	0.744 (0.678-0.803)	2 ³
BW, 12-leads	0.603 (0.531-0.671)*	2 ⁵
DFA1, 12-leads	0.600 (0.528-0.668)*	2 ⁴
DFA2, 12-leads	0.545 (0.474-0.616)*	2 ⁴
DF, 12-leads	0.634 (0.563-0.701)§	2 ⁵
MAA, 12-leads	0.721 (0.654-0.782)§	2 ³
MDF, 12-leads	0.615 (0.544-0.683)§	2 ⁷
MDS, 12-leads	0.727 (0.659-0.787)§	2 ¹
OI, 12-leads	0.641 (0.570-0.707)§	2 ³
PSA, 12-leads	0.743 (0.677-0.802)§	2 ²

* Inferior to C-statistic of AMSA model (DeLong method p<0.006 after Bonferroni correction)

§ Statistically not different from the C-statistic of AMSA model

Figure S1. Representation of the organization index. The organization index was calculated as the ratio between the summed power of the bandwidth of the fundamental and its harmonic peaks, and the total power.

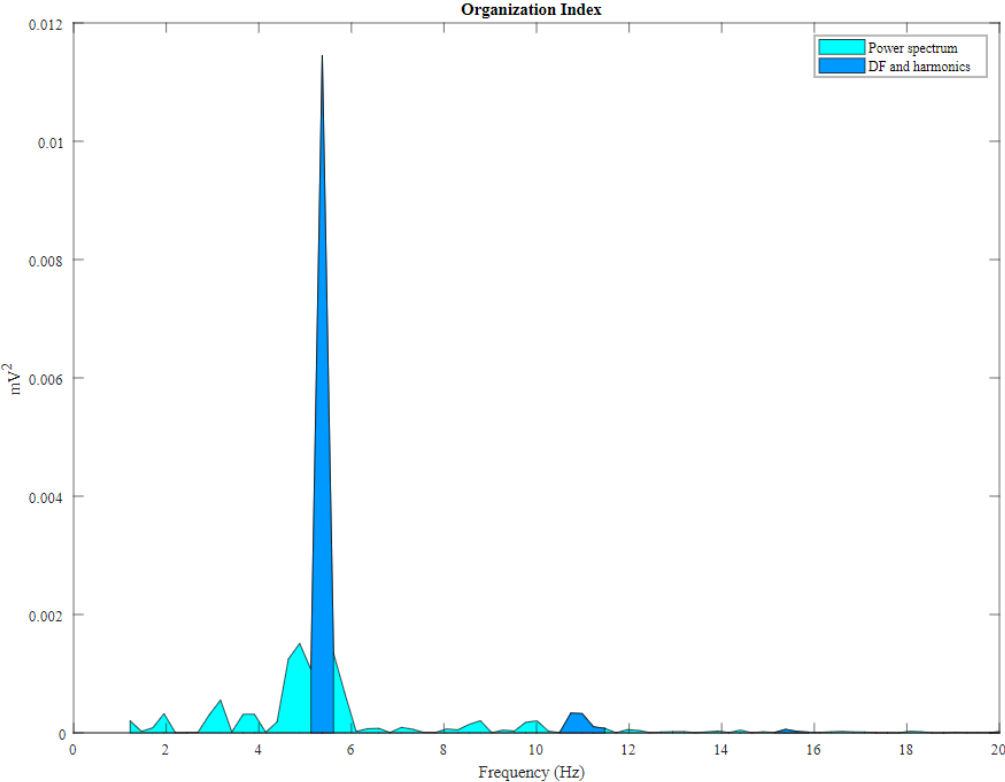


Figure S2. Stepwise process of detrended fluctuation analysis.

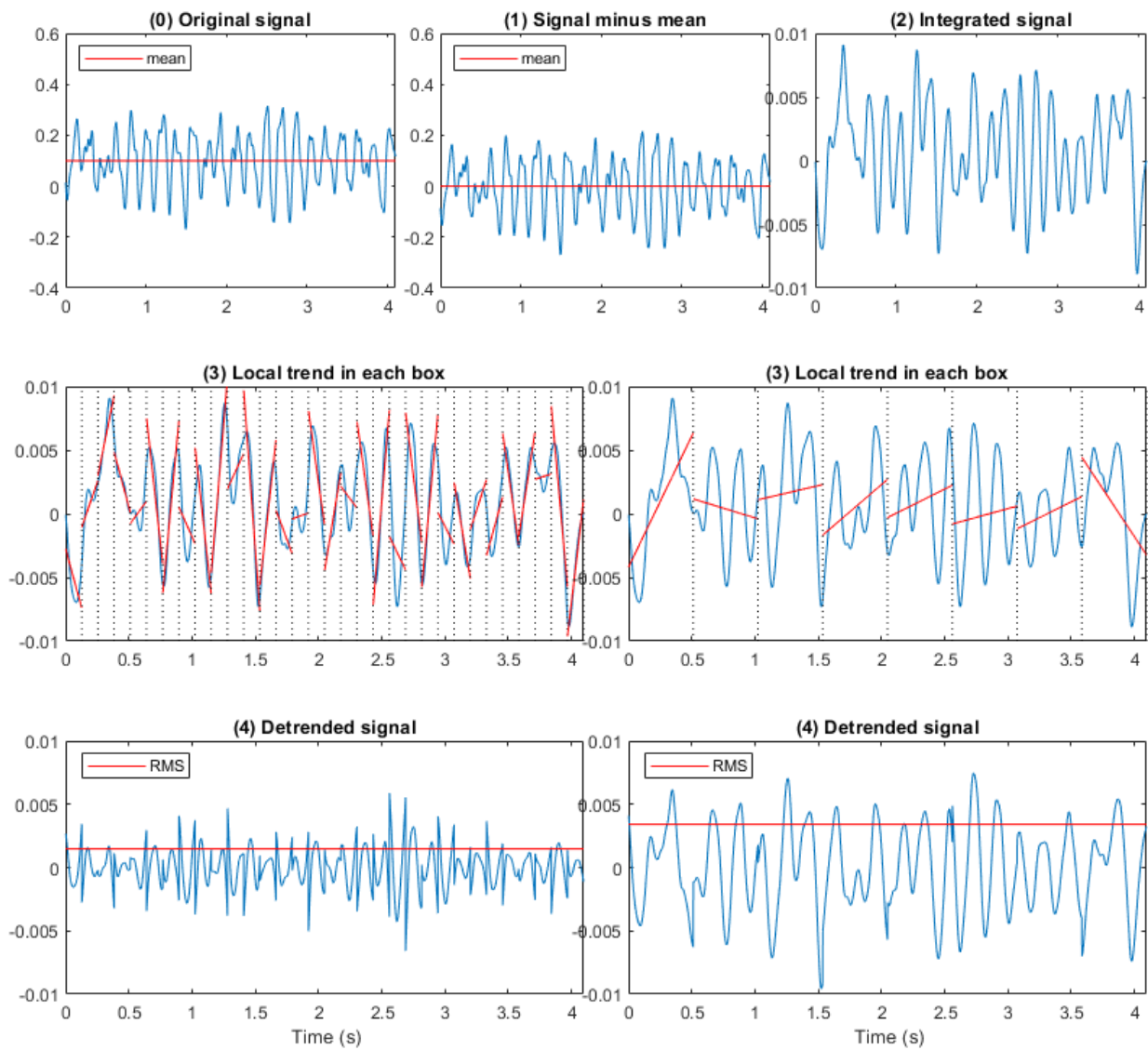


Figure S3. Two scaling exponents of detrended fluctuation analysis (DFA α 1 and DFA α 2). The red lines represent the scaling exponents as obtained from the DFA analysis. DFA α 1 is defined as the DFA scaling exponent on small time scales, i.e. 0.004 to 0.128 seconds; DFA α 2 is defined as the DFA scaling exponent on larger time scales, i.e. 0.128 to 4.0 seconds.

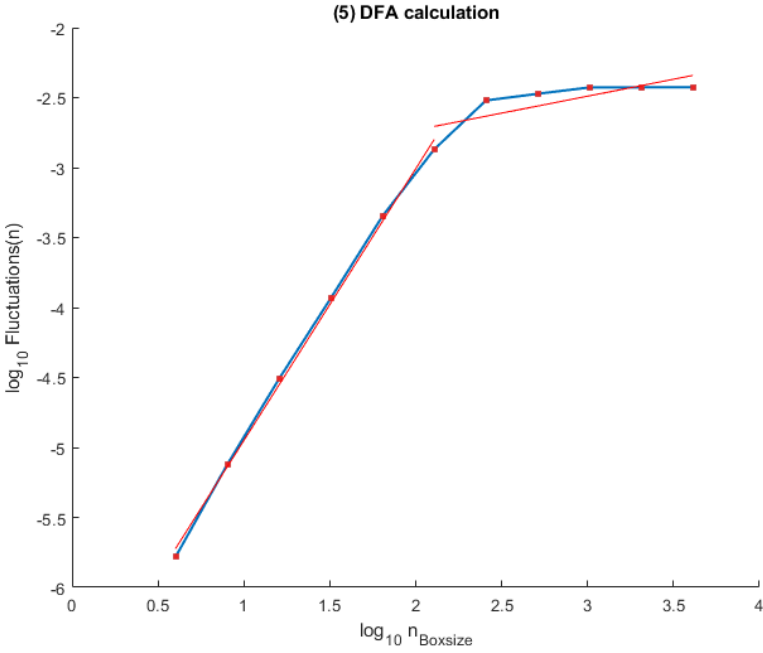


Figure S4. Optimization of the regularization parameter C of the support vector machine models. Overview of the obtained C-statistics for all chosen values of the regularization parameter C. The red dot represents the optimal value of C per VF-characteristic.

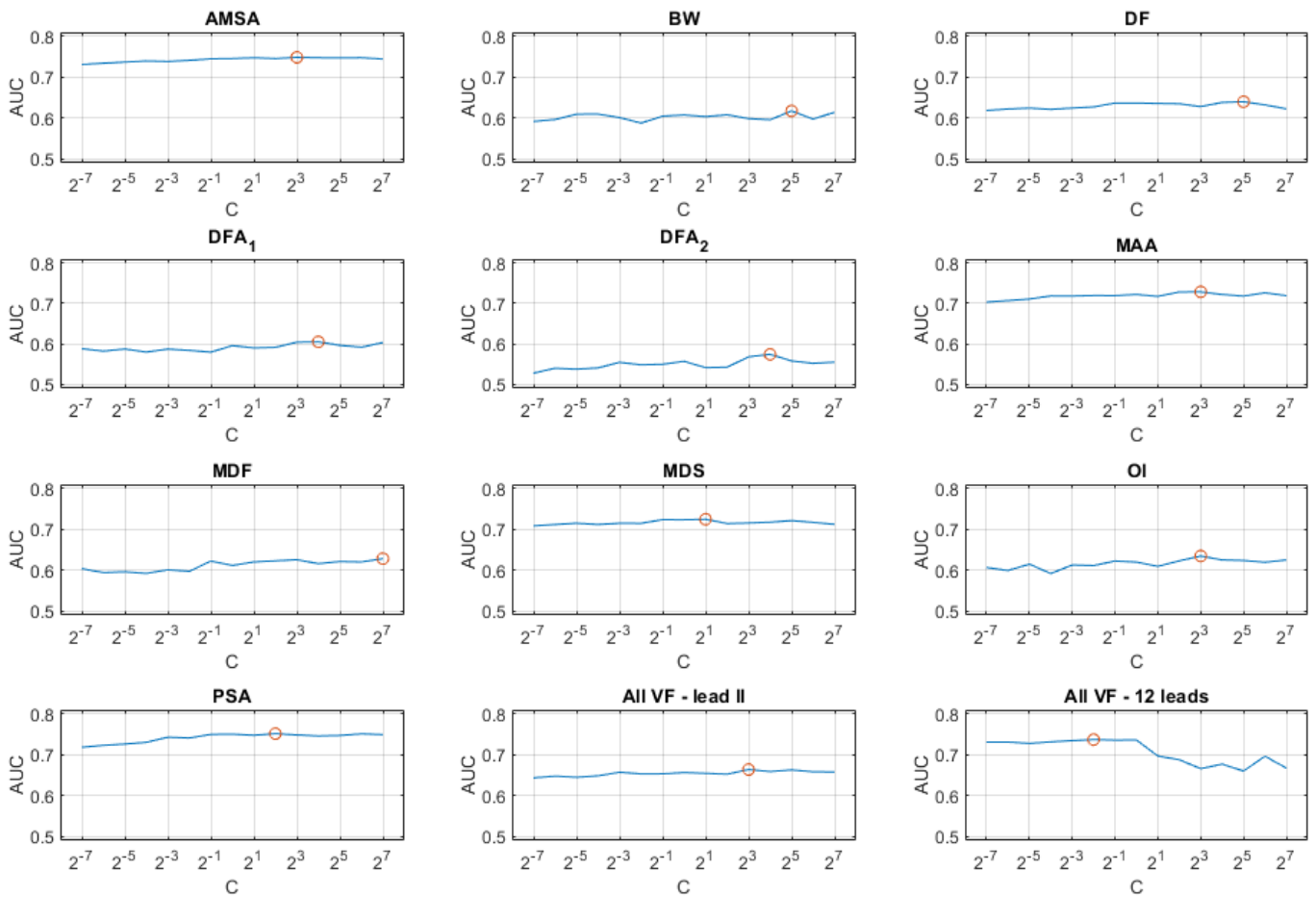


Figure S5. Flowchart of the support vector machine process.

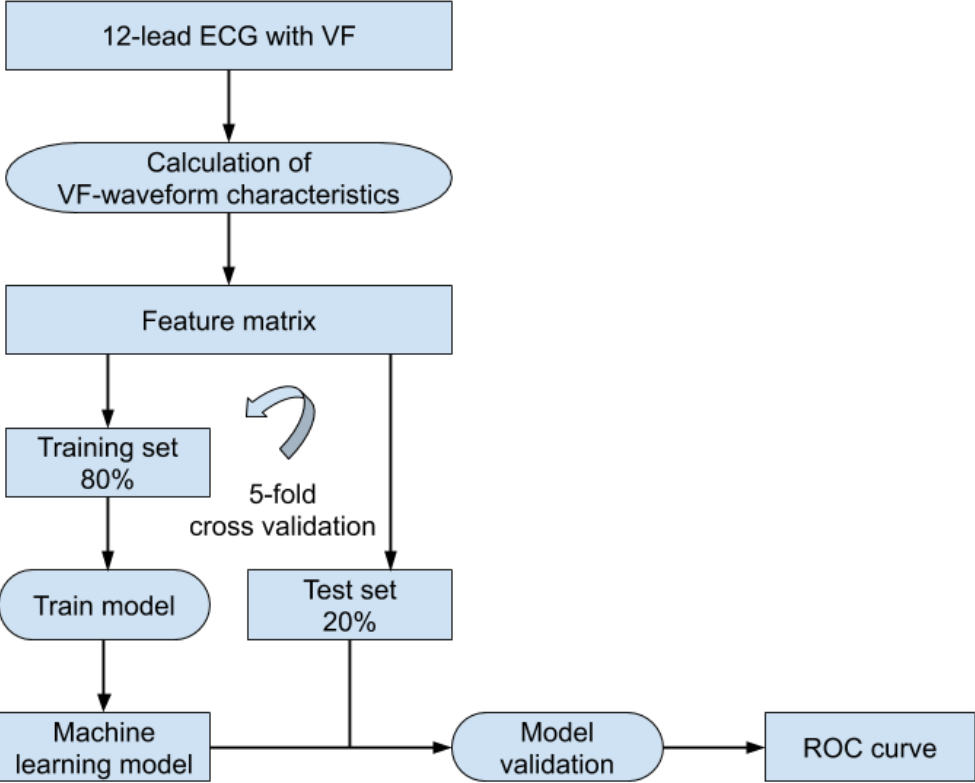
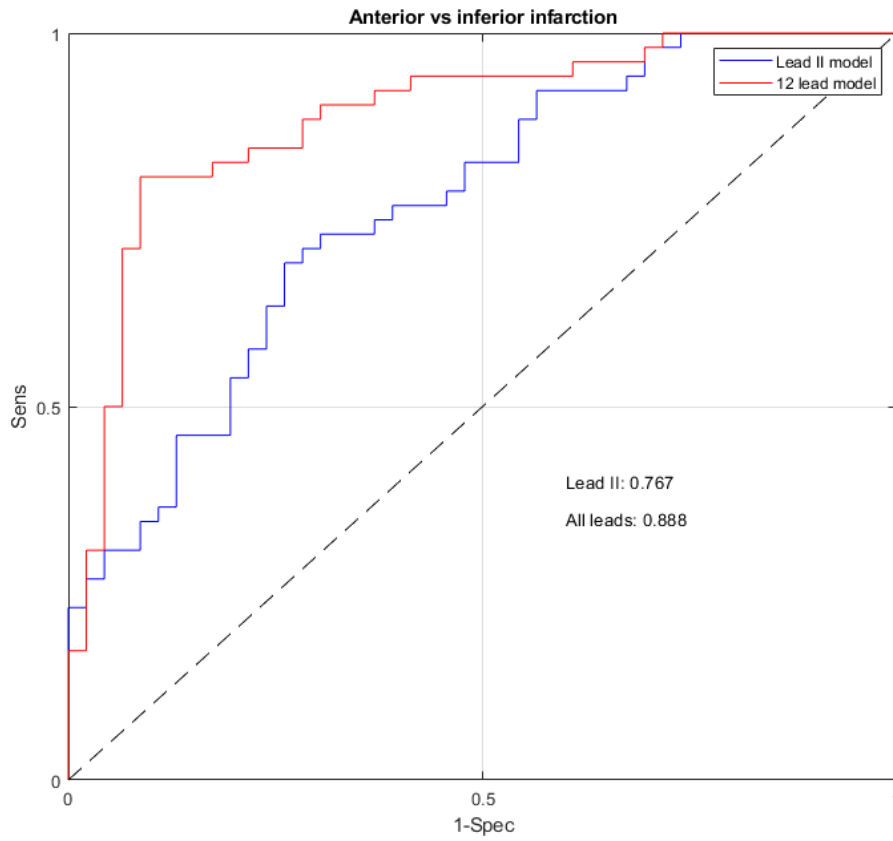


Figure S6. Ancillary analysis on infarct localization. ROC curves of anterior vs inferior myocardial infarction, all VF characteristics combined in a single lead (blue, C= 2-6) or multiple lead (red, C=20) SVM model.



	Lead II model	12-lead model	p-value (DeLong method)
ROC analysis	0.767 (0.671-0.847)	0.888 (0.809-0.943)	0.0096
PPV*	74%	83%	

* to identify an inferior MI